



**HAL**  
open science

# A pH-triggered self-releasing humic acid hydrogel loaded with porcine interferon $\alpha/\gamma$ achieves anti-pseudorabies virus effects by oral administration

Maoyuan Sun, Yongli Shi, Baishi Lei, Wuchao Zhang, Jingjing Feng, Shenghu Ge, Wanzhe Yuan, Kuan Zhao

## ► To cite this version:

Maoyuan Sun, Yongli Shi, Baishi Lei, Wuchao Zhang, Jingjing Feng, et al.. A pH-triggered self-releasing humic acid hydrogel loaded with porcine interferon  $\alpha/\gamma$  achieves anti-pseudorabies virus effects by oral administration. *Veterinary Research*, 2024, 55 (1), pp.153. 10.1186/s13567-024-01411-w . hal-04801067

**HAL Id: hal-04801067**

**<https://hal.science/hal-04801067v1>**

Submitted on 25 Nov 2024

**HAL** is a multi-disciplinary open access archive for the deposit and dissemination of scientific research documents, whether they are published or not. The documents may come from teaching and research institutions in France or abroad, or from public or private research centers.


L'archive ouverte pluridisciplinaire **HAL**, est destinée au dépôt et à la diffusion de documents scientifiques de niveau recherche, publiés ou non, émanant des établissements d'enseignement et de recherche français ou étrangers, des laboratoires publics ou privés.

RESEARCH ARTICLE

Open Access



# A pH-triggered self-releasing humic acid hydrogel loaded with porcine interferon $\alpha/\gamma$ achieves anti-pseudorabies virus effects by oral administration

Maoyuan Sun<sup>1</sup>, Yongli Shi<sup>2</sup>, Baishi Lei<sup>1</sup>, Wuchao Zhang<sup>1</sup>, Jingjing Feng<sup>1</sup>, Shenghu Ge<sup>3</sup>, Wanzhe Yuan<sup>1\*</sup> and Kuan Zhao<sup>1\*</sup> 

## Abstract

Interferon  $\alpha$  (IFN $\alpha$ ) and interferon  $\gamma$  (IFN $\gamma$ ) play pivotal roles in mediating crucial biological functions, including anti-viral activity and immune regulation. However, the efficacy of monomeric IFN is limited, and its administration relies solely on injection. To address this issue, we successfully expressed and purified a recombinant porcine IFN $\alpha$  and IFN $\gamma$  fusion protein (rPoIFN $\alpha/\gamma$ ). Furthermore, we developed a pH-triggered humic acid hydrogel delivery system that effectively protects rPoIFN $\alpha/\gamma$  from gastric acid degradation, enhancing its oral bioavailability. Neither the humic acid hydrogel nor rPoIFN $\alpha/\gamma$  exhibited cytotoxic effects on porcine kidney-15 (PK-15) cells in vitro. The replication of vesicular stomatitis virus and pseudorabies virus (PRV) was effectively inhibited by rPoIFN $\alpha/\gamma$ , resulting in an antiviral activity of approximately  $10^4$  U/mL. Scanning electron microscopy revealed that the humic acid hydrogel had a loose and porous honeycomb structure. The IFN $\alpha/\gamma$ @PAM<sup>gel</sup> hydrogel effectively adsorbed rPoIFN $\alpha/\gamma$ , as confirmed by Fourier transform infrared spectroscopy analysis, demonstrating a favourable IFN-loading capacity. In vitro experiments revealed that IFN $\alpha/\gamma$ @PAM<sup>gel</sup> swelled and released IFN $\alpha/\gamma$  rapidly at pH 7.4 but not at pH 1.2. The oral administration of IFN $\alpha/\gamma$ @PAM<sup>gel</sup> in mice enhanced the proliferation and differentiation of CD4<sup>+</sup> and CD8<sup>+</sup> cells. Additionally, mice infected with PRV and treated with IFN $\alpha/\gamma$ @PAM<sup>gel</sup> presented increased transcription levels of interferon-stimulated genes in the serum, reduced mortality rates, lower viral loads in various tissues, and decreased levels of organ damage. In conclusion, this study demonstrates that orally administered IFN $\alpha/\gamma$ @PAM<sup>gel</sup> has antiviral and immunomodulatory effects, highlighting its potential as a therapeutic agent against PRV infection.

**Keywords** rPoIFN $\alpha/\gamma$ , pH-sensitive hydrogels, PRV, oral drug delivery system

Handling editor: Marie Galloux.

\*Correspondence:

Wanzhe Yuan

yuanwanzhe@126.com

Kuan Zhao

zhaokuan519@126.com

<sup>1</sup> College of Veterinary Medicine, Hebei Agricultural University, Baoding, China

<sup>2</sup> College of Pharmacy, Xinxiang Medical University, Xinxiang, China

<sup>3</sup> Hebei Mingzhu Biotechnology Co., Ltd., Xingtai, China

## Introduction

Pseudorabies, also known as Aujeszky's disease, is a highly pathogenic infectious disease caused by the pseudorabies virus (PRV) [1]. PRV is an enveloped virus with a linear double-stranded DNA genome of approximately 143 kb that encodes more than 70 proteins [2]. PRV can infect a wide range of mammalian species, including pigs, sheep, dogs, and rodents. The only natural host for PRV is pigs, and infection in pregnant sows leads to



© The Author(s) 2024. **Open Access** This article is licensed under a Creative Commons Attribution 4.0 International License, which permits use, sharing, adaptation, distribution and reproduction in any medium or format, as long as you give appropriate credit to the original author(s) and the source, provide a link to the Creative Commons licence, and indicate if changes were made. The images or other third party material in this article are included in the article's Creative Commons licence, unless indicated otherwise in a credit line to the material. If material is not included in the article's Creative Commons licence and your intended use is not permitted by statutory regulation or exceeds the permitted use, you will need to obtain permission directly from the copyright holder. To view a copy of this licence, visit <http://creativecommons.org/licenses/by/4.0/>. The Creative Commons Public Domain Dedication waiver (<http://creativecommons.org/publicdomain/zero/1.0/>) applies to the data made available in this article, unless otherwise stated in a credit line to the data.

reproductive disorders such as spontaneous abortion and stillbirth, resulting in significant economic losses in the pig industry [3, 4]. Since 2011, PRV variant strains have been identified in China and have resulted in vaccination failure [5, 6]. More importantly, studies have shown that PRV can be transmitted to humans and cause respiratory dysfunction, neurological disorders, and conjunctivitis [7, 8]. Therefore, PRV infection may be a threat to public and human health.

Interferons (IFNs) are pivotal in immune regulation and are crucial cytokines in the host antiviral defence mechanism [9]. Three distinct classes of IFNs have been identified: type I (IFN $\alpha$ , IFN $\beta$ , IFN $\epsilon$ , IFN $\kappa$ , and IFN $\omega$ ), type II (IFN $\gamma$ ), and type III (IFN $\lambda$ ) [10]. However, IFN- $\nu$  has recently been found in the vertebrate genome sequence. These findings suggest that type IV interferons may be present [11]. Among these IFNs, type I IFNs, particularly IFN $\alpha$ , demonstrate broad-spectrum antiviral activities against various viruses compared with other IFN types. IFN $\gamma$ , the only type II IFN, is pivotal in innate and adaptive immunity against viral and intracellular bacterial infections [12–14]. Porcine IFN (PoIFN)- $\alpha$  and - $\gamma$  have been extensively utilized in the treatment and prophylaxis of viral diseases. For example, they are employed to treat animal diseases caused by transmissible gastroenteritis viruses and African swine fever virus [15, 16]. However, several challenges persist in the utilization of IFN. For example, single-component IFNs lack the dual functionality of antiviral and immunomodulatory effects. Furthermore, the administration of protein drugs, primarily via injection, poses significant stress on animals and is difficult to perform, thereby severely restricting the utilization of IFNs.

Hydrogels are synthesized through covalent or non-covalent interactions between diverse polymeric materials and have been extensively investigated because their distinctive properties, including biocompatibility, permeability, and wettability, resemble those of human tissues [17–19]. Humus has been extensively utilized in the medical and veterinary fields because of its antiviral, antibacterial, and anti-inflammatory properties [20–22]. Humic acid (HA), a derivative of humus, is an organic substance generated through the decomposition of animals and plants. It constitutes approximately 50% of the Earth's natural organic carbon reservoirs, which are extensively distributed across terrestrial soils, rivers, lakes, and marine environments [23–25]. Because HA hydrogels exhibit ultralow systemic toxicity, they are also used as carriers for cancer treatment [26]. In recent years, researchers have discovered that incorporating hydrophobic moieties can increase the stability of hydrogels. HA molecules possess both hydrophobic and active functional groups, making them promising candidates for the

fabrication of hydrogels [27–30]. Because HA is rich in adsorption sites, the adsorption properties of the hydrogels can be further enhanced [31]. Therefore, the utilization of HA for hydrogel modification represents a highly promising strategy. The natural proteinaceous macromolecule gelatin (Gel), derived from collagen denaturation as a byproduct of meat production, has been deemed safe by the US Food and Drug Administration (FDA) [32]. Gels are widely employed in the fabrication of synthetic hydrogels, and researchers have successfully integrated them with humus to yield 3D hydrogels that exhibit significantly enhanced bactericidal properties [33, 34]. The raw materials potassium humate (KHA) and Gel can be utilized along with acrylamide (AM), 2-acrylamido-2-methyl-1-propanesulfonic acid (AMPS), *N,N'*-methylene bisacrylamide (MBA), and potassium persulfate (KPS) to fabricate pH-sensitive HA hydrogels through aqueous polymerization.

The present study investigated the expression of IFN $\alpha$  and  $\gamma$  fusion protein (IFN $\alpha/\gamma$ ) as a strategic approach to enhance the antiviral and immune regulatory efficacy of IFN. To enable the oral administration of IFN $\alpha/\gamma$ , we prepared HA hydrogels loaded with IFN $\alpha/\gamma$  (IFN $\alpha/\gamma$ @PAM<sup>gel</sup>) (Figure 1). The safety and efficacy of the generated IFN $\alpha/\gamma$ @PAM<sup>gel</sup> were evaluated both *in vitro* and *in vivo*. These results will help promote the development of highly effective IFN drugs and oral delivery systems to help prevent and treat pseudorabies.

## Materials and methods

### Reagents, cells, viruses, and animals

The gelatin was procured from Sigma Biotechnology Co., Ltd. (USA). The chemicals AM (99% purity), KPS (99.5% purity), AMPS (98% purity), MBA (analytical grade), and KHA (70% purity) were purchased from Shanghai Macklin Biochemical Co., Ltd. (China). Anti-mouse CD4, FITC (Clone: GK1.5) and anti-mouse CD8 $\alpha$ , PE (Clone: 53–6.7) antibodies were obtained from Hangzhou Multi Sciences Biotechnology Co., Ltd. (China). DH5 $\alpha$  and BL21(DE3) bacteria were procured from Beijing Quanshi Gold Biotechnology Co., Ltd. (China). PK-15 and African green monkey kidney (Vero) cells were cultured in Dulbecco's modified Eagle's medium (DMEM) supplemented with 10% fetal bovine serum (Gibco, Thermo Fisher Scientific, Waltham, MA, USA). The cells were maintained at 37 °C in 5% CO<sub>2</sub>. The PRV variant strain HB1201 was isolated in our laboratory [35]. Six-week-old BALB/c mice were purchased from Beijing Huafukang Biotechnology Co., Ltd. (China).

### Expression and purification of recombinant PoIFN $\alpha/\gamma$

The coding sequences for porcine IFN $\alpha$  (accession no. KF414740.1) and IFN $\gamma$  (accession no. NM213948.1)

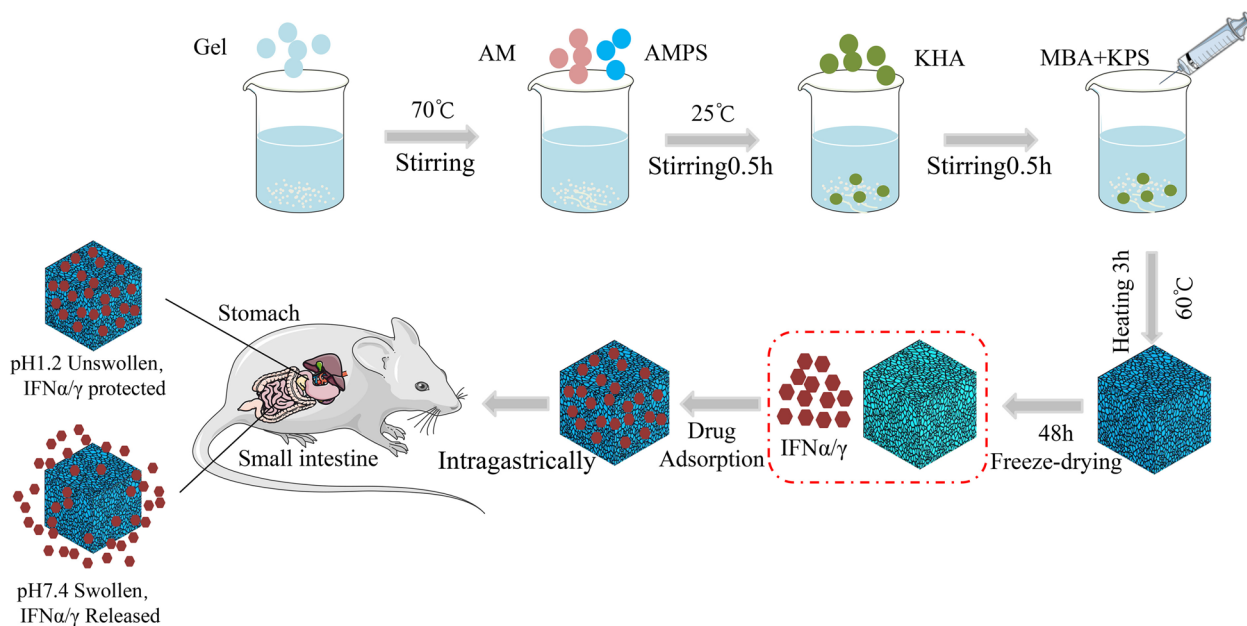


**Figure 1** Schematic representation of the rPoIFN $\alpha/\gamma$  release pattern at pH 1.2 (stomach) and pH 7.4 (intestine) and the hydrogel synthesis route. rPoIFN $\alpha/\gamma$ , recombinant porcine interferon  $\alpha$  and  $\gamma$  fusion protein.

were analysed and optimized with NanoPro and JCat. The signal peptide sequences were removed. The optimized sequence was connected using a flexible linker (GGGGSGGGSGGGGS) that was synthesized and cloned and inserted into the pET28a vector. The rPoIFN $\alpha/\gamma$  protein was expressed and purified following previously established protocols, and the expression of recombinant proteins in the form of inclusion bodies is very common. The purified recombinant proteins can be made biologically active by refolding in refolding buffer at 4 °C for 48 h, which has been used in many other studies [36, 37]. The purity of the isolated rPoIFN $\alpha/\gamma$  was assessed by SDS-PAGE and western blotting. The primary antibody used was a mouse anti-His mAb, and the secondary antibody used was horseradish peroxidase (HRP)-coupled goat anti-mouse IgG (Biodragon Biotechnology Co., Ltd., China). The concentration of purified rPoIFN $\alpha/\gamma$  was determined using a BCA protein assay kit, and the lipopolysaccharide in the recombinant protein was eliminated with an endotoxin removal kit. (Solarbio, Beijing, China), following the manufacturer's instructions. The purified rPoIFN $\alpha/\gamma$  was stored at -80 °C for long-term preservation.

#### Determination of rPoIFN $\alpha/\gamma$ cytotoxicity

The cytotoxicity of rPoIFN $\alpha/\gamma$  was assessed using a Cell Counting Kit-8 (CCK-8) assay (Solarbio) following the manufacturer's instructions. PK-15 cells were seeded in 96-well plates and grown to 90% confluence. PK-15 cells

were used to evaluate the cytotoxicity of the drug. This is a common research method used in many other similar studies [38, 39]. In accordance with the fourfold dilution method, 300  $\mu$ L of rPoIFN $\alpha/\gamma$  (0.8 mg/mL) was diluted with 900  $\mu$ L of DMEM containing 2% foetal bovine serum, resulting in a total of seven dilution gradients; eight repetitions were used for each gradient. Subsequently, 100  $\mu$ L of diluted protein was added to each well. Following a 24 h incubation period, 10  $\mu$ L of CCK-8 was added, and the mixture was incubated at 37 °C for 2 h. The absorbance at 450 nm was subsequently measured using a microplate reader.

#### Determination of the antiviral activity of rPoIFN $\alpha/\gamma$ in vitro

As previously described, the antiviral activities of rPoIFN $\alpha/\gamma$  were assessed using a cytopathic effect (CPE) inhibition assay involving vesicular stomatitis virus (VSV) and PRV in Vero and PK-15 cells [40]. Briefly, when the cells in the 96-well plates reached 90% confluence, they were treated with 100  $\mu$ L of rPoIFN $\alpha/\gamma$  at fourfold serial dilutions for 16 h, followed by incubation with VSV or PRV (100 TCID<sub>50</sub>/well). Eight wells without virus were used as negative controls, and eight wells with virus but no rPoIFN $\alpha/\gamma$  were used as positive controls. The active titre of rPoIFN $\alpha/\gamma$  was determined after 48 h using the Reed-Muench method [41].

### Preparation of pH-sensitive hydrogels

pH-responsive hydrogels were synthesized via aqueous solution polymerization. AM, AMPS, MBA, and KPS were combined and dissolved in 10 mL of deionized water. Subsequently, 0.1 g of KHA was dissolved in 10 mL of deionized water and stirred well with the gel mixture for 30 min to achieve a homogeneous suspension, which was then incubated at 60 °C for 3 h. The resulting products were thoroughly rinsed with deionized water and ethanol three times to remove unreacted monomers and obtain purified hydrogels. The wet hydrogels were lyophilized using a SCIENTZ-10 N vacuum freeze drier (Ningbo SCIENTZ Science and Technology Corporation, China). The hydrogel without cargo was designated PAM<sup>gel</sup>. An aliquot of dry hydrogel was immersed in a solution of IFN $\alpha/\gamma$  at 4 °C for 12 h. The IFN-loaded hydrogel was designated IFN $\alpha/\gamma$ @PAM<sup>gel</sup>.

### Characterization of pH-sensitive hydrogels

The morphology and structural characteristics of the hydrogels were observed by scanning electron microscopy (SEM, Phenom Pro microscope, USA) with an accelerating voltage of 15 kV [42]. Fourier transform infrared spectroscopy (FT-IR) was performed on the hydrogels and interferon solutions via an FT-IR spectrometer (PerkinElmer, China). The samples were subjected to differential scanning calorimetry (DSC) analysis using a TA Instruments system at a scanning rate of 10 °C/min across a 50 °C–300 °C temperature range. The cytotoxicity of the hydrogels was assessed using established protocols as previously described [43, 44]. The swelling properties of the cargo-free PAM<sup>gel</sup> were assessed using a previously established methodology [45].

### rPoIFN $\alpha/\gamma$ release studies

In vitro drug release studies were conducted by immersing an aliquot of the IFN-loaded hydrogel in simulated gastric fluid (pH 1.2) or intestinal fluid (pH 7.4). The mixture was incubated at 37 °C with rotational mixing at 100 rpm. At specific time intervals (0, 4, 8, 12, 16, 20, and 24 h), an aliquot (0.5 mL) was sampled for detection. An equal volume of fresh buffer solution was subsequently added to restore the initial volume. The release of IFN in the solution was determined by measuring the absorbance at 280 nm using UV/VIS spectrophotometry [46, 47].

### Intestinal safety and CD4<sup>+</sup> and CD8<sup>+</sup> T-cell assessments

A total of 24 6-week-old female BALB/c mice were randomly allocated into two groups: the IFN $\alpha/\gamma$ @PAM<sup>gel</sup> treatment group and the phosphate-buffered saline (PBS) control group. The IFN $\alpha/\gamma$ @PAM<sup>gel</sup> treatment group received an oral administration of IFN adsorbed by the

hydrogel at a dose of 100  $\mu$ g/mouse for three consecutive days, whereas the control group was administered an equivalent volume of PBS. The peripheral blood and spleen tissues of the mice in each experimental group were collected at specific time points (1, 3, 5, and 7 days) following drug administration. The levels of CD4<sup>+</sup> and CD8<sup>+</sup> T cells and interferon-stimulated gene (ISG) transcription were subsequently quantified. Each assay contained at least 100  $\mu$ L of peripheral blood sample and was labelled with the corresponding antibodies. Immediately after sample preparation, flow cytometry (FCM) was used for prompt detection and analysis (Attune NxT, Thermo Fisher Scientific, USA) [48]. After the mice were treated for three days, the duodenum was fixed with a 10% formalin solution, followed by tissue section preparation and subsequent evaluation of intestinal safety.

### Quantitative reverse transcription polymerase chain reaction (qRT-PCR)

To evaluate the capacity of IFN $\alpha/\gamma$ @PAM<sup>gel</sup> to induce ISG production in mice, the expression of the three ISGs in the spleen was analysed. Total RNA was extracted from the spleen tissue via TRIzol RNA extraction reagent (Takara Bio Inc., Japan). The Pkr, Ifit1, and Isg20 levels were quantified via TaqMan real-time PCR. Relative expression levels were determined via the  $2^{-\Delta\Delta C_t}$  method. To standardize the values for each sample,  $\beta$ -actin mRNA was used as an internal control. The primers utilized for the ISGs are shown in Table 1.

### Determination of anti-PRV activity in vivo

Thirty 6-week-old BALB/c female mice were randomly allocated to PRV infection, IFN $\alpha/\gamma$ @PAM<sup>gel</sup> treatment, or PBS control groups. The challenge dose was determined on the basis of previously reported findings [49–52]. Mice in the PRV infection and IFN $\alpha/\gamma$ @PAM<sup>gel</sup> treatment groups were intramuscularly infected with 200

**Table 1** Primers used for gene cloning and qPCR analysis

Primers	Nucleotide sequence (5' → 3')
Mouse-PKR-F	ATGCACGGAGTAGCCATTACG
Mouse-PKR-R	TGACAATCCACCTTGTTTTCGT
Mouse-IFIT1-F	TACAGGCTGGAGTGTGCTGAGA
Mouse-IFIT1-R	CTCCACTTTCAGAGCCTTCGCA
Mouse-ISG20-F	CTTGGGCCTCAAAGGGTGAG
Mouse-ISG20-R	CGGGTCGGATGTACTTGTCA
Mouse- $\beta$ -actin-F	CATTGCTGACAGGATGCAGAAGG
Mouse- $\beta$ -actin-R	TGCTGGAAGTGGACAGTGAGG
PRV-rtgB-F	GTCACCTTGTGGTTGTTG
PRV-rtgB-R	CCACATCTACTACAAGAACG

$\mu\text{L}$  of PRV at a titre of  $10^{2.5}$  TCID<sub>50</sub>. The IFN $\alpha/\gamma$ @PAM<sup>gel</sup> treatment group received an oral administration of interferon adsorbed by the hydrogel at a dose of 100  $\mu\text{g}/\text{mouse}$  for three consecutive days, starting 12 h after the challenge. The PBS control group remained uninfected with PRV and did not receive treatment with IFN $\alpha/\gamma$ @PAM<sup>gel</sup>. All surviving mice were euthanized 14 days post-treatment (dpt), after which the spleen, lungs, and brain were collected. Tissues from the mice that died during the experiment were collected immediately after death. Viral DNA was extracted from tissue sections. The number of viral DNA copies was determined via qPCR [53]. The primers used in this study are shown in Table 1.

### Statistical analysis

The statistical analyses were conducted using GraphPad Prism 6 (GraphPad Software Inc., La Jolla, CA, USA). Statistical significance was assessed using Student's *t* tests. A value of  $p < 0.05$  indicated statistical significance.

## Results

### Expression and purification of rPoIFN $\alpha/\gamma$

The coding sequences of rPoIFN $\alpha$  and rPoIFN $\gamma$  were optimized and linked using a flexible linker. The tandem fusion sequence of rPoIFN $\alpha$  and rPoIFN $\gamma$  (rPoIFN $\alpha/\gamma$ ) is presented in Additional file 1. The rPoIFN $\alpha/\gamma$  sequence was subsequently cloned and inserted into the pET28a vector, which was subsequently transformed into BL21(DE3) cells for expression. The findings of this study indicate that the expression of rPoIFN $\alpha/\gamma$  occurred in the form of inclusion bodies. The rPoIFN $\alpha/\gamma$  was purified with Ni-agarose resin. The SDS-PAGE results revealed

a major band with a molecular weight of 40 kDa (Figure 2A), which was verified to be tagged by western blotting with an anti-His antibody (Figure 2B). Thus, rPoIFN $\alpha/\gamma$  was expressed and purified at high concentrations for subsequent experimental use.

### Cytotoxicity and antiviral activity of rPoIFN $\alpha/\gamma$ in vitro

The cytotoxicity of rPoIFN $\alpha/\gamma$  was evaluated in PK-15 cells using the CCK-8 assay. Compared with that of untreated control cells, the viability of rPoIFN $\alpha/\gamma$ -treated PK-15 cells was significantly lower at dilutions ranging from  $4^{-1}$  to  $4^{-2}$  (Figure 2C). The viability of PK-15 cells remained unaffected by dilutions ranging from  $4^{-3}$  to  $4^{-7}$ . These findings validate the safety profile of rPoIFN $\alpha/\gamma$  in PK-15 cells, establishing a foundation for subsequent investigations. The antiviral activities of rPoIFN $\alpha/\gamma$  were determined using the CPE inhibition method. PK-15 cells were incubated with dilutions of rPoIFN $\alpha/\gamma$  for 12 h and subsequently infected with either PRV or VSV. The results demonstrated that the antiviral activity of rPoIFN $\alpha/\gamma$  against VSV and PRV was approximately  $10^4$  U (mg/mL) (Figure 2D). These findings demonstrated that rPoIFN $\alpha/\gamma$  effectively suppressed the replication of VSV and PRV in PK-15 cells.

### SEM and cytotoxicity assay of the hydrogels

As shown in Figure 3A, the structural characteristics of the cargo-free PAM<sup>gel</sup> were examined using SEM, revealing a honeycomb-like appearance at various magnifications ( $\times 300$ ,  $\times 400$ ,  $\times 600$ , and  $\times 800$ ). These dispersed network structures can function as efficient drug carriers, offering robust drug loading and release support. After calculation, the porosity of the cargo-free PAM<sup>gel</sup>

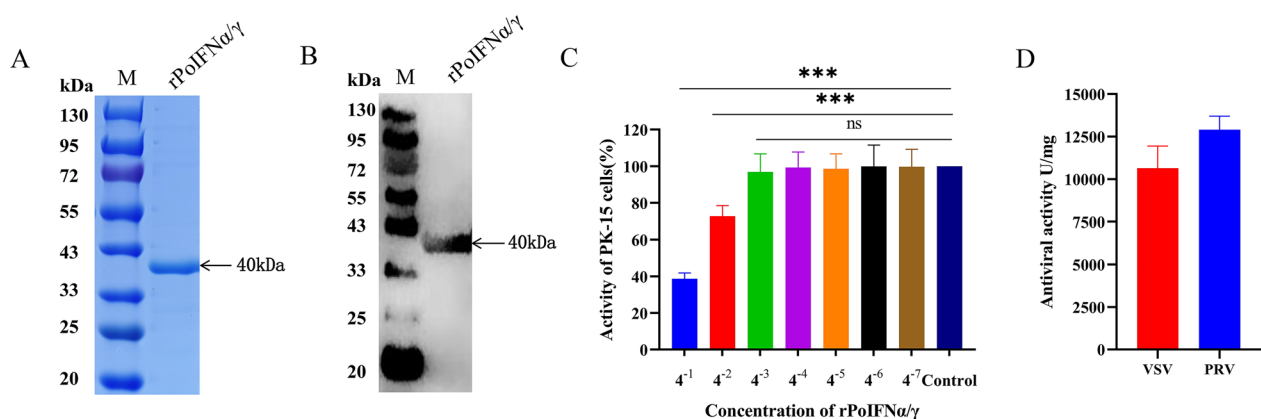


**Figure 2** Expression, purification, toxicity assessment, and antiviral activity evaluation of the rPoIFN $\alpha/\gamma$  recombinant protein. **A**

SDS-PAGE analysis of the purified rPoIFN $\alpha/\gamma$  protein. **B** Western blot analysis of the rPoIFN $\alpha/\gamma$  protein. **C** Cytotoxicity of various concentrations of rPoIFN $\alpha/\gamma$  on PK-15 cells was assessed after 24 h of incubation. Statistical significance was determined using Student's *t* tests ( $***p < 0.001$ ; ns, not significant). **D** Antiviral activity of rPoIFN $\alpha/\gamma$  against vesicular stomatitis virus (VSV) and pseudorabies virus (PRV) was assessed in vitro using the cytopathic effect inhibition method.

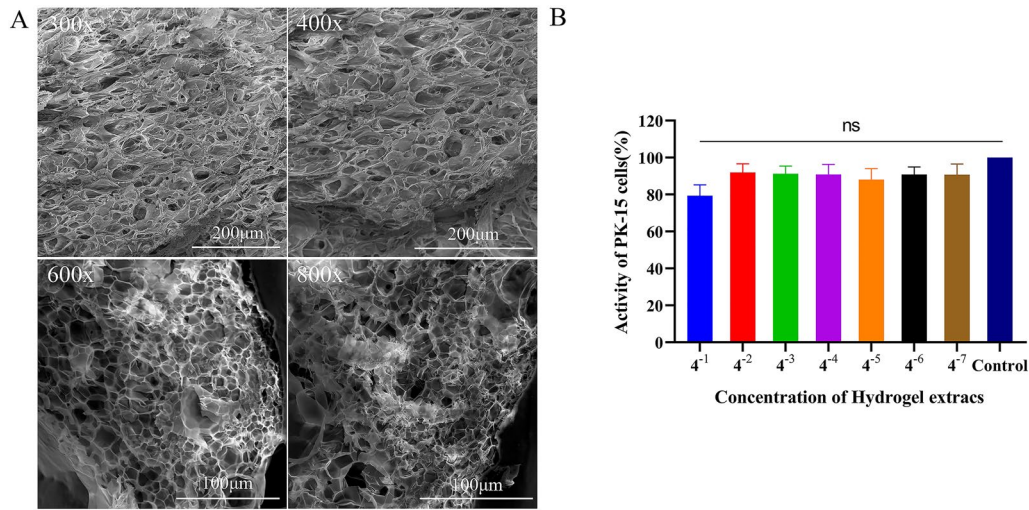


**Figure 3** SEM images at different magnifications and toxicity evaluation of hydrogels. **A** SEM images of the hydrogels were captured at various magnifications, including  $\times 300$ ,  $\times 400$ ,  $\times 600$ , and  $\times 800$ . **B** Cytotoxicity of the hydrogel extracts at various concentrations against PK-15 cells after incubation for 24 h.

**Table 2** Toxicity scores of the hydrogel extracts

Score	RGR (%)
0	$\geq 100$
1	75 ~ 99
2	50 ~ 74
3	25 ~ 49
4	1 ~ 24

RGR = (OD of test group / OD of control group)  $\times$  100%.

was determined to be  $60.1 \pm 8.89\%$  (Additional file 2). To further verify the safety of the hydrogels, the cytotoxicity of the cargo-free PAM<sup>gel</sup> was determined using a cytotoxicity assay (CCK-8). The results revealed that after the cells were incubated with different concentrations of the extracts for 24 h, the cell viability was greater than 75%

(Figure 3B). This level was classified as level 1 according to the corresponding evaluation criteria (Table 2). There was almost no toxicity to cells. These results preliminarily confirmed the safety of the hydrogels as drug carriers and provided a rationale for subsequent animal experiments.

**FT-IR and DSC analyses**

FT-IR and DSC analyses are viable methods for investigating drug-hydrogen atom interactions. In the FT-IR spectrum of the cargo-free PAM<sup>gel</sup> (Figure 4A), the absorption bands observed at  $3420\text{ cm}^{-1}$  and  $1645\text{ cm}^{-1}$  may be caused by the stretching vibrations of the hydroxyl and carbonyl groups. In the amide II region, a distinct peak at  $1548\text{ cm}^{-1}$  was observed for both IFN $\alpha/\gamma$  and IFN $\alpha/\gamma$ @PAM<sup>gel</sup>, indicating the presence of a natural helical structure and protein aggregates. Furthermore, the absence of this characteristic peak in the cargo-free PAM<sup>gel</sup> confirms the successful loading of interferon onto

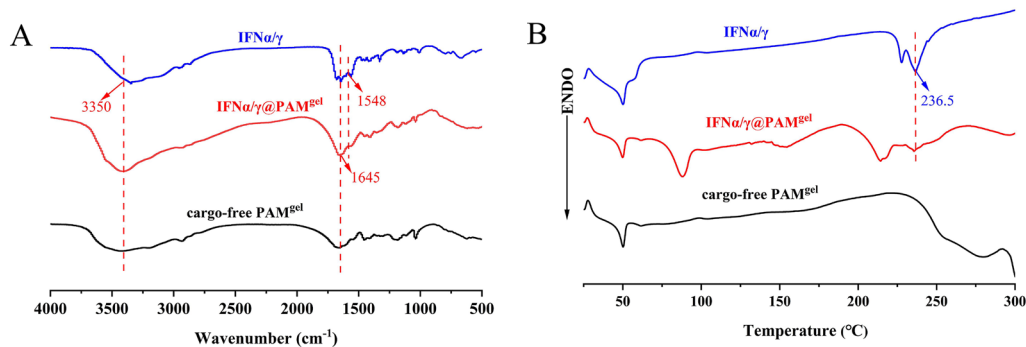


**Figure 4** FT-IR and DSC analysis of IFN $\alpha/\gamma$ , IFN $\alpha/\gamma$ @PAM<sup>gel</sup>, and PAM<sup>gel</sup>. **A** FT-IR spectra. **B** DSC spectra.

the hydrogel. The distribution of IFN $\alpha/\gamma$  in the hydrogel was also investigated. The DSC patterns of IFN $\alpha/\gamma$ , cargo-free PAM<sup>gel</sup>, and IFN $\alpha/\gamma$ @PAM<sup>gel</sup> are shown in Figure 4B. An endothermic peak was observed in the DSC pattern of free IFN $\alpha/\gamma$ , which was caused by the fusion of IFN $\alpha/\gamma$  crystals. In contrast, the observed peak in the DSC pattern of IFN $\alpha/\gamma$ @PAM<sup>gel</sup> exhibited a noticeable decrease. This phenomenon suggested that most of the IFN $\alpha/\gamma$  distributed in IFN $\alpha/\gamma$ @PAM<sup>gel</sup> had an amorphous or molecular state, which improved the bioavailability and release rates of the encapsulated IFN $\alpha/\gamma$ .

#### Swelling behavior of hydrogels and IFN $\alpha/\gamma$ release studies

To mimic the swelling behavior of hydrogels and the release of IFN $\alpha/\gamma$  in the gastric and intestinal environments, *in vitro* experiments were conducted at pH 1.2 and 7.4, respectively. After 24 h of immersion, the maximal swelling values were recorded as  $1122.7 \pm 109.7\%$  (pH=1.2 PBS) and  $2112.1 \pm 181.2\%$  (pH=7.4 PBS) (Figure 5A). These findings suggest enhanced delivery of drug molecules within the slightly alkaline environment (e.g., the intestinal tract). The results also revealed that the release of IFN $\alpha/\gamma$  from the hydrogel had a typical pH dependence. After 24 h of incubation, only  $16.4 \pm 0.1\%$  of the IFN $\alpha/\gamma$  was released at pH 1.2 in PBS. In contrast,  $82.3 \pm 0.3\%$  of the IFN $\alpha/\gamma$  was released at pH 7.4 in PBS (Figure 5B; \*\*\*,  $p < 0.001$ ). On the basis of these release profiles, we speculated that IFN $\alpha/\gamma$ @PAM<sup>gel</sup> could deliver more IFN $\alpha/\gamma$  molecules into the intestinal tract and prevent IFN $\alpha/\gamma$  leakage in the stomach. This process effectively protects IFN $\alpha/\gamma$  from enzymatic degradation by pepsin, thereby increasing the bioavailability of IFN $\alpha/\gamma$ .

#### IFN $\alpha/\gamma$ @PAM<sup>gel</sup> has no adverse effects on the duodenum

The duodenum is the main absorption site in the body of an animal. Damage to the intestinal villi or epithelium

severely affects the absorption of substances. To evaluate the safety of IFN $\alpha/\gamma$ @PAM<sup>gel</sup> in the duodenum, the mice were orally administered IFN $\alpha/\gamma$ @PAM<sup>gel</sup> for three consecutive days. The toxicity of IFN $\alpha/\gamma$ @PAM<sup>gel</sup> was then evaluated on the basis of the degree of pathological damage to the duodenum tissue of the mice. Histopathological examination of the duodenums of the mice in both the oral IFN $\alpha/\gamma$ @PAM<sup>gel</sup> and PBS groups revealed no evidence of pathological damage (Figures 6A and B). Moreover, the density and length of the intestinal villi were essentially the same in the IFN $\alpha/\gamma$ @PAM<sup>gel</sup> and PBS groups. Thus, the safety of IFN $\alpha/\gamma$ @PAM<sup>gel</sup> in the duodenum of mice has been established, confirming its suitability as a secure delivery vector for oral drug administration systems.

#### Orally administered IFN $\alpha/\gamma$ @PAM<sup>gel</sup> promotes the proliferation of CD4<sup>+</sup> and CD8<sup>+</sup> T lymphocytes *in vivo*

IFN $\gamma$  has immunomodulatory effects, and consequently, the effects of IFN $\alpha/\gamma$ @PAM<sup>gel</sup> on the proliferation of CD4<sup>+</sup> and CD8<sup>+</sup> T lymphocytes in peripheral blood were investigated by FCM. The results revealed that the numbers of CD4<sup>+</sup> and CD8<sup>+</sup> T lymphocytes were significantly greater in the IFN $\alpha/\gamma$ @PAM<sup>gel</sup> group (Figures 7E–H) than in the PBS group (Figures 7A–D). Furthermore, there was no discernible difference in CD4<sup>+</sup> levels between the IFN $\alpha/\gamma$ @PAM<sup>gel</sup> and PBS groups after one day of oral administration. However, a significant difference was observed at 3 and 5 days post-administration (Figure 7I,  $p < 0.001$ ). Seven days after oral administration, the number of CD4<sup>+</sup> T lymphocytes in the IFN $\alpha/\gamma$ @PAM<sup>gel</sup> oral group decreased but was still greater than that in the PBS group (Figure 7I,  $p < 0.05$ ). The levels of CD8<sup>+</sup> T lymphocytes in the IFN $\alpha/\gamma$ @PAM<sup>gel</sup> group were significantly different from those in the PBS group throughout the experiment (Figure 7J,  $p < 0.001$ ,  $p < 0.05$ ). These findings suggest that the oral administration of

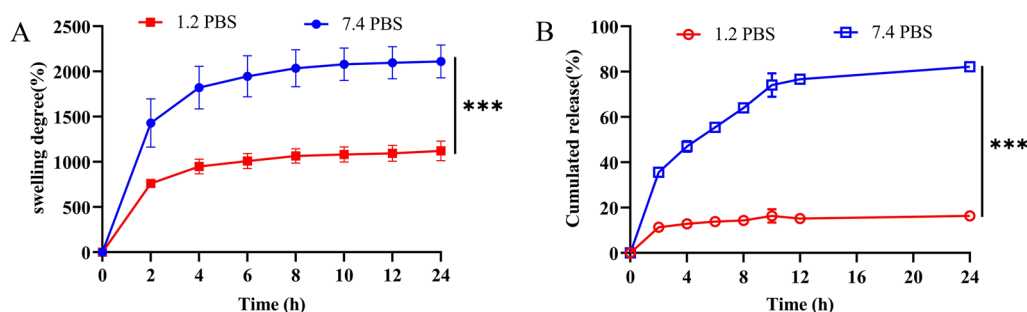


**Figure 5** Swelling behavior of hydrogels and cumulative drug release in buffers at different pH values. **A** Swelling behavior of hydrogels in buffers at pH 1.2 and 7.4. **B** Cumulative release of rPolIFN $\alpha/\gamma$  from hydrogels in different pH conditions representing gastric fluid (pH 1.2) and intestinal fluid (pH 7.4) at 37 °C. The results are the mean  $\pm$  standard deviation ( $n=3$ ).



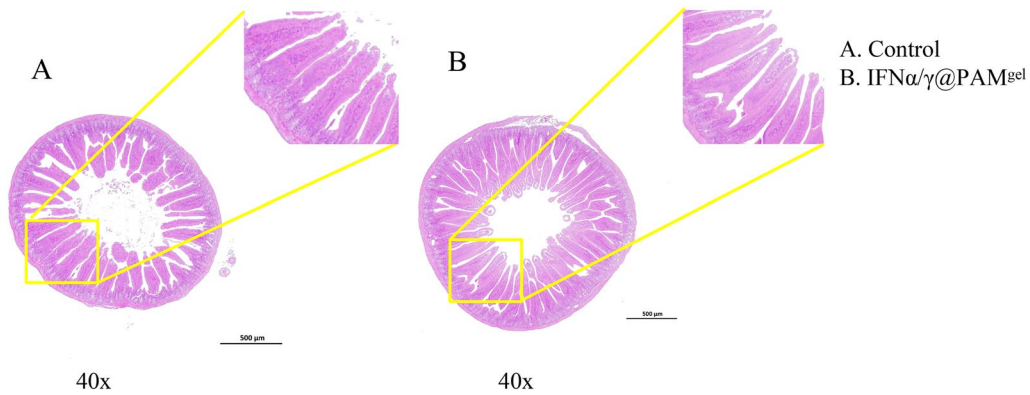


**Figure 6** Pathological changes in mouse duodenal tissue. Three days after dosing, the toxicity of IFN $\alpha/\gamma$ @PAM<sup>9el</sup> was evaluated according to the degree of pathological damage to the mouse duodenal tissue. **A** Histopathological observation of haematoxylin–eosin (H&E)-stained sections from the control group. **B** Histopathological observation of haematoxylin–eosin (H&E)-stained sections from the IFN $\alpha/\gamma$ @PAM<sup>9el</sup> group.

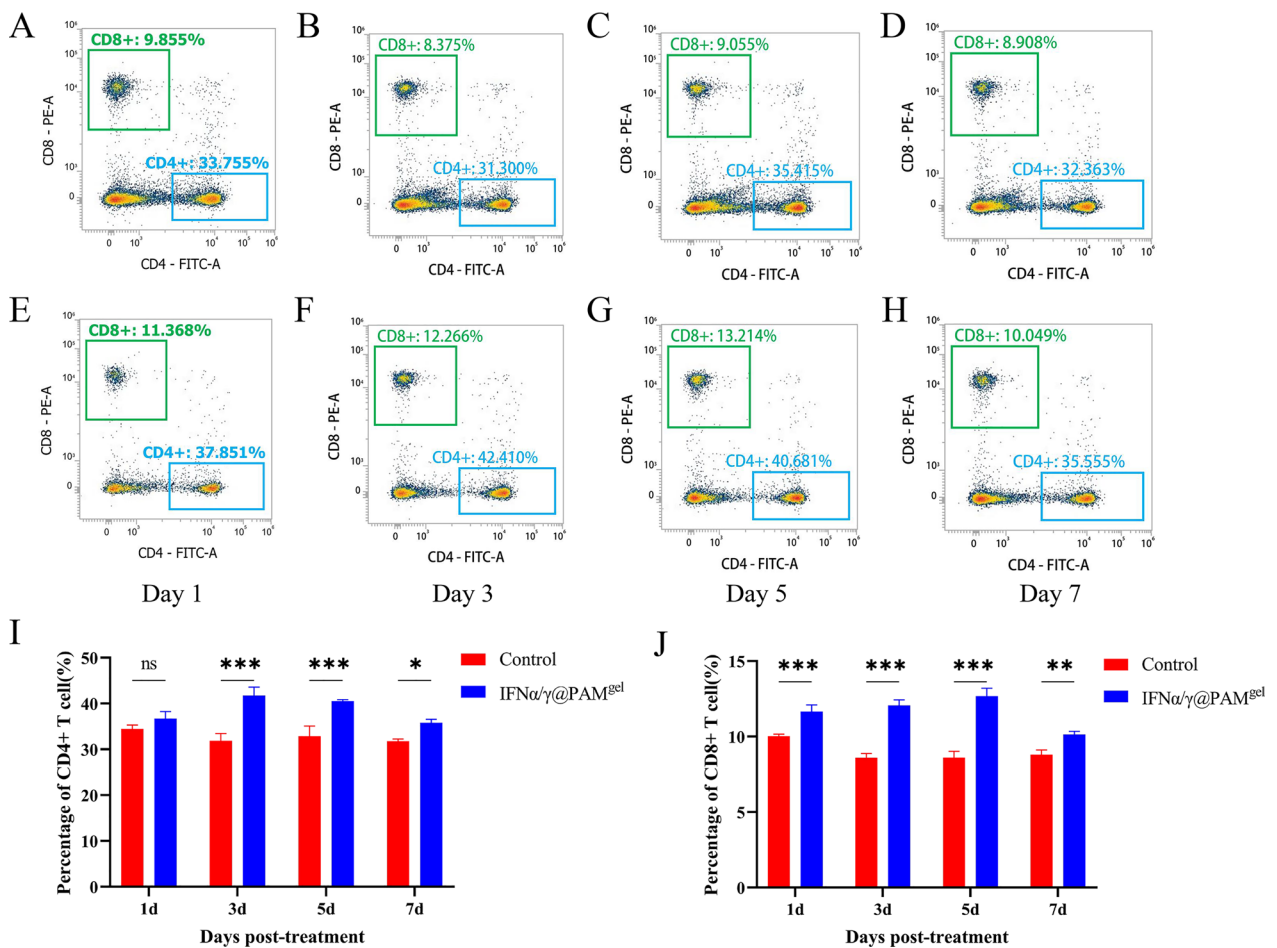


**Figure 7** Analysis of CD<sub>4</sub><sup>+</sup> and CD<sub>8</sub><sup>+</sup> T cells in the blood of experimental mice. **A–H** Changes in CD<sub>4</sub><sup>+</sup> and CD<sub>8</sub><sup>+</sup> T-cell levels on day 1, 3, 5, and 7 in mice in the oral IFN $\alpha/\gamma$ @PAM<sup>9el</sup> group and control group. **I–J** Ratios of CD<sub>4</sub><sup>+</sup> and CD<sub>8</sub><sup>+</sup> T cells. **I** CD<sub>4</sub><sup>+</sup> levels showed no difference after one day of oral administration between IFN $\alpha/\gamma$ @PAM<sup>9el</sup> and the PBS control groups but showed a significant difference 3 to 7 days after administration. (\* $p < 0.05$ ; \*\*\* $p < 0.001$ ; ns, not significant). **J** There was a significant increase in the ratio of CD<sub>8</sub><sup>+</sup> T cells in the IFN $\alpha/\gamma$ @PAM<sup>9el</sup> group compared with that in the control group from 1 to 7 days. (\*\* $p < 0.01$ ; \*\*\* $p < 0.001$ ).

IFN $\alpha/\gamma$ @PAM<sup>gel</sup> can increase the proliferation of CD4<sup>+</sup> and CD8<sup>+</sup> T lymphocytes in vivo.

#### IFN $\alpha/\gamma$ @PAM<sup>gel</sup> induces the expression of ISGs in vivo

To further validate the impact of the oral administration of IFN $\alpha/\gamma$ @PAM<sup>gel</sup> on the innate immune response in the host, we extracted mRNA samples from mouse spleens to perform qRT-PCR analysis of three ISGs (*Pkr*, *Ifit1*, and *Isg20*). The results revealed that the ISG levels in the IFN $\alpha/\gamma$ @PAM<sup>gel</sup> treatment group were significantly greater than those in the PBS group at 3 and 5 days post-treatment (Figures 8A–C,  $p < 0.001$ ). The ISG mRNA upregulation peaked three days post-treatment at approximately eightfold, with a significant difference compared with that in the control group ( $p < 0.001$ ). Up to 7 days post-treatment, the mRNA levels of the different ISGs in the IFN $\alpha/\gamma$ @PAM<sup>gel</sup> treatment group were still greater than those in the control group, albeit not significantly. The findings of this study demonstrate that

the oral administration of IFN $\alpha/\gamma$ @PAM<sup>gel</sup> elicits in vivo induction of ISG expression.

#### IFN $\alpha/\gamma$ @PAM<sup>gel</sup> inhibits PRV infection and decreases the tissue viral load in vivo

To further assess the therapeutic efficacy of oral IFN $\alpha/\gamma$ @PAM<sup>gel</sup> against viral infections, we employed PRV-infected mice as an experimental model for treatment. PRV-infected mice in the untreated group presented characteristic clinical symptoms, including pruritus, scratching, gnawing of the facial skin, skin lesions accompanied by tissue damage and bleeding, and neurological symptoms (data not shown). The mice in the untreated group started dying at 4 dpt, and all the mice had died by 8 dpt (Figure 9A). The mice in the oral IFN $\alpha/\gamma$ @PAM<sup>gel</sup> treatment group presented milder clinical symptoms than did those in the untreated group. The mice that received oral IFN $\alpha/\gamma$ @PAM<sup>gel</sup> exhibited mortality starting at 5 dpt, with a recorded survival rate of 70%

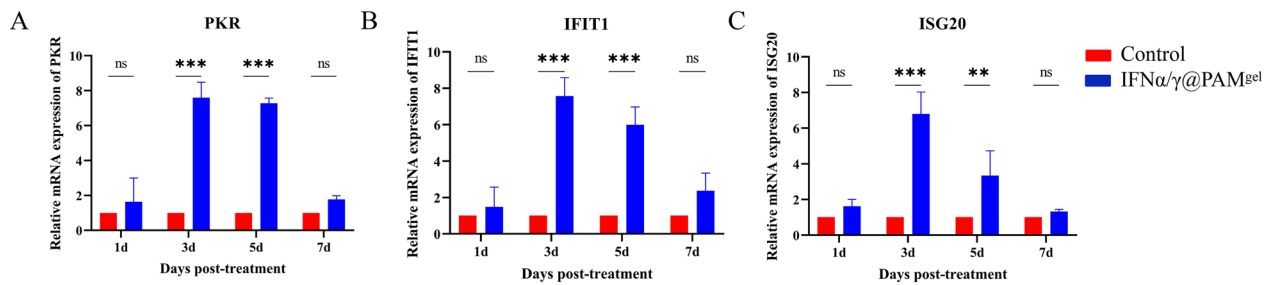


**Figure 8** IFN $\alpha/\gamma$ @PAM<sup>gel</sup> induced ISG (*Pkr*, *Ifit1*, and *Isg20*) expression in mice. The spleens were collected at the indicated time points. RT-qPCR analysis of *Pkr* (A), *Ifit1* (B), and *Isg20* (C) mRNA in mice from the fresh spleen samples of the IFN $\alpha/\gamma$ @PAM<sup>gel</sup> and control groups collected on days 1, 3, 5, and 7. Mice in the treatment group were administered IFN $\alpha/\gamma$ @PAM<sup>gel</sup> orally for three days, and the controls were untreated. Total RNA from the spleen tissue was extracted using RNA Plus reagent and reverse transcribed into cDNA. Relative gene expression analysis was performed using the  $2^{-\Delta\Delta Ct}$  method, and  $\beta$ -actin was used as an endogenous control. The data are representative of three independent experiments analysed by Student's *t* tests (\*\* $p < 0.01$ ; \*\*\* $p < 0.001$ ; ns, not significant).

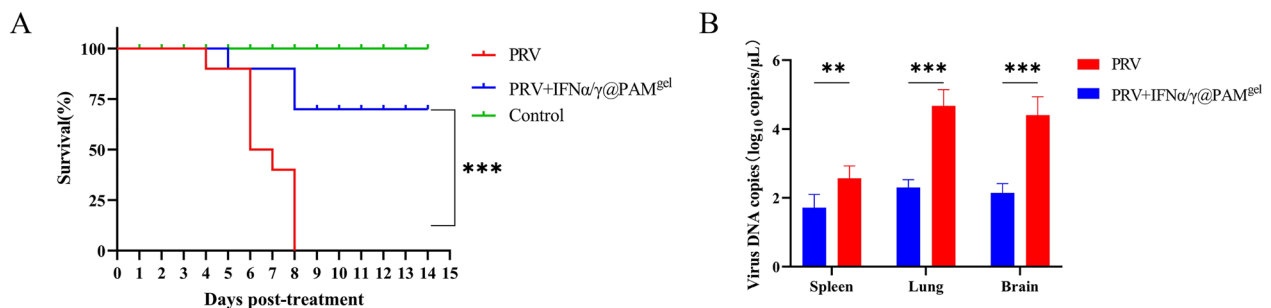


**Figure 9** Protective efficacy of IFN $\alpha/\gamma$ @PAM<sup>gel</sup> against PRV infection in mice. **A** Survival rates of mice after challenge. **B** Viral DNA copies in different tissues (spleen, lung, and brain). Viral DNA copies were quantified for each tissue using qPCR and calculated as viral DNA copies per microliter. The data are presented as the mean  $\pm$  standard deviation from three experiments. The statistical significance of differences between IFN $\alpha/\gamma$ @PAM<sup>gel</sup>-treated and untreated groups was determined using Student's *t* tests (\*\* $p < 0.01$ ; \*\*\* $p < 0.001$ ; ns, not significant).

(Figure 9A). All the mice in the control group survived and appeared to be in a good mental state. To further investigate the impact of IFN $\alpha/\gamma$ @PAM<sup>gel</sup> on PRV replication in vivo, we quantified the viral DNA copy number in various tissues (spleen, lung, and brain) via qPCR. The results revealed a significant reduction in the PRV DNA copy number in the spleen, brain, and lung tissue of the IFN $\alpha/\gamma$ @PAM<sup>gel</sup>-treated group compared with that in the untreated group, with a decrease of approximately 2.0 log units. (Figure 9B,  $p < 0.01$  and  $p < 0.001$ ). The findings of this study suggest that the use of hydrogels as carriers for recombinant IFN $\alpha/\gamma$  protein has potential for ameliorating clinical symptoms, preventing PRV-related mortality, and effectively suppressing PRV replication in diverse tissues and organs.

#### IFN $\alpha/\gamma$ @PAM<sup>gel</sup> reduces PRV-induced pathological damage

PRV infection can cause tissue and organ damage. To evaluate this, tissue samples from the lungs, spleen, and brain of mice in different experimental groups were collected for comparative analysis. The findings revealed that mice infected with PRV in the untreated group presented pronounced hemorrhaging in their brains, spleens, and lungs. The brain, spleen, and lung tissue samples analysed from the mice in the IFN $\alpha/\gamma$ @PAM<sup>gel</sup> treatment group exhibited characteristics comparable to those of the control group and did not exhibit evident pathological damage (Figure 10A). In addition, the histopathological results revealed that the brain pyramidal cells were wrinkled and that the boundary between the nucleus and cytoplasm was indistinct in the untreated

group. Furthermore, the spleen and lung tissue samples in the untreated group exhibited extensive congestion, accompanied by perivascular edema and loose arrangement of the connective tissue; the spleen also exhibited lymphocyte necrosis and dilation of the medullary sinus. In the treatment group, only minor local hemorrhaging and alveolar wall thickening were occasionally observed (Figure 10B). The control group exhibited intact tissue structures with distinct boundaries. These findings demonstrate the protective effect of the oral administration of IFN $\alpha/\gamma$ @PAM<sup>gel</sup> against PRV-induced pathological damage in infected mice.

#### Discussion

Here, we present an effective potential treatment with antiviral and immunomodulatory effects on PRV. This treatment uses a hydrogel as a delivery carrier of IFN to produce an antiviral effect via oral administration. Using hydrogels as an oral drug delivery system is one method to protect protein drugs from destruction by stomach acid [54, 55]. Our experiments demonstrated that the fusion protein rPoIFN $\alpha/\gamma$  can inhibit PRV replication in vitro. Furthermore, the prepared hydrogel carrier performed excellently in in vitro experiments. To comprehensively evaluate the prophylactic and therapeutic effects of IFN $\alpha/\gamma$ @PAM<sup>gel</sup> on pseudorabies in mice, we investigated the clinical, pathological, viral load, and immunological changes in mice infected with PRV after treatment with and without IFN $\alpha/\gamma$ @PAM<sup>gel</sup>. Our results showed that IFN $\alpha/\gamma$ @PAM<sup>gel</sup> induces ISG expression in mice. The clinical symptoms of pseudorabies and tissue damage caused by PRV infection were also alleviated.

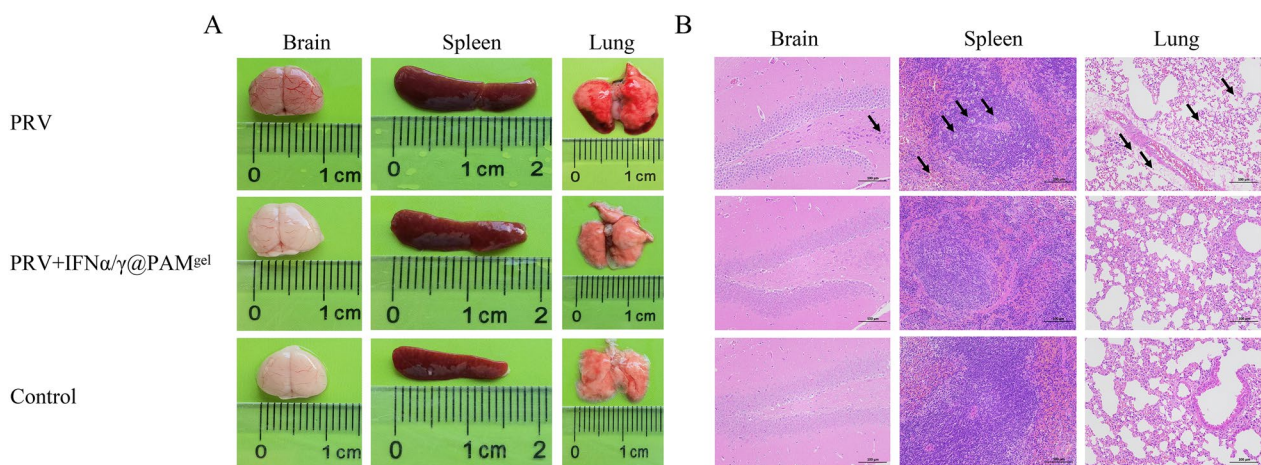


**Figure 10** Pathological changes in mouse organs (brain, spleen, and lung). **A** Representative photographs of the appearance of the whole organs of mice from the PRV, PRV + IFN $\alpha/\gamma$ @PAM<sup>gel</sup>, and control groups. **B** Histopathological observation of hematoxylin–eosin (H&E)-stained brain, spleen, and lung sections from each group of mice. PRV, pseudorabies virus-infected; PRV + IFN $\alpha/\gamma$ @PAM<sup>gel</sup>, pseudorabies virus-infected and orally administered humic acid hydrogel loaded with interferon  $\alpha$  and  $\gamma$  fusion protein.

Previous studies have focused primarily on individual IFN family members, including IFN $\alpha$ , IFN $\lambda$ , IFN $\gamma$ , and IFN $\delta$  [41, 56–58]. Partial mixtures of IFNs from different family members can exert synergistic effects, but not all of them can [36]. Additionally, the production process is further complicated by the requirement of expressing two or more proteins, even if a combination of IFN family members has a synergistic effect. Our previous studies revealed that the expression of IFN $\alpha$  and IL-2 fusion proteins combines their functions and prolongs their effects [59]. These findings reveal the potential of tandem proteins generated through gene fusion to exhibit dual functionalities within a single molecule. On the basis of this premise, we created a recombinant IFN $\alpha$  and IFN $\gamma$  fusion protein using a flexible linker region, which enabled us to validate its *in vivo* and *in vitro* anti-PRV activity. The results showed that the rPoIFN $\alpha/\gamma$  fusion protein could be expressed and purified and had no obvious toxic effects on cells. In addition, the recombinant protein showed strong antiviral activity against both VSV and PRV (Figure 2D), which was greater than that of monomeric IFN alone (data not shown). Therefore, our strategy of using a fusion protein is feasible. Nevertheless, in our study, the recombinant protein still had certain limitations. For example, the expression of this protein occurs in the form of inclusion bodies, resulting in reduced biological activity compared with that of soluble proteins. In this study, the appropriate concentration of recombinant PoIFN $\alpha/\gamma$  was tested, and the results revealed that 1.0 g/L was the minimum concentration that completely inhibited PRV *in vitro* (Additional file 3). In follow-up experiments, we will attempt to improve the antiviral activity of the IFN fusion protein by changing the expression system, optimizing the expression conditions, and reducing the potential adverse effects caused by factors such as dose.

The development of hydrogels dates back to 1960. Since then, hydrogels have been widely used in the field of drug delivery research for slow drug release, especially for oral drug delivery systems [60]. Oral administration is convenient and has little impact on animals, which is convenient for large-scale use. The efficacy of protein drugs is compromised upon their entry into the digestive tract due to their susceptibility to degradation by stomach acid and enzymes, leading to therapeutic failure. To solve this problem, we investigated a pH-sensitive hydrogel that acts as a carrier for IFN $\alpha/\gamma$  (IFN $\alpha/\gamma$ @PAM<sup>gel</sup>) and prevents its destruction by stomach acids and enzymes. The synthesized polymeric hydrogel in this study is nontoxic and has a three-dimensional network structure (Figure. 3), enabling efficient absorption and retention of substantial amounts of water or biological

fluids. Moreover, the intestine is the main site of nutrient and drug absorption. Therefore, the duodenum was chosen for the safety evaluation. The results revealed that no pathological injury occurred in the duodenal histopathology of the mice in the oral IFN $\alpha/\gamma$ @PAM<sup>gel</sup> group (Figure 6B), and we believe that IFN $\alpha/\gamma$ @PAM<sup>gel</sup> is safe for the body, which aligns with findings reported in previous studies [61, 62]. Additionally, the synthesized hydrogel exhibited pronounced pH-responsive characteristics (Figure 5A), with notably superior expansion performance observed under slightly alkaline conditions compared with that observed under acidic conditions [45, 55]. The release profile also demonstrated that the prepared hydrogel exhibited pH-dependent control over IFN $\alpha/\gamma$  release (Figure 5B), thereby enhancing the bioactivity of orally administered IFN $\alpha/\gamma$  [54]. The absorption bands of the cargo-free PAM<sup>gel</sup> (Figure 4A) at 3420 cm<sup>-1</sup> and 1645 cm<sup>-1</sup> in the FT-IR spectra may be caused by the stretching vibrations of -OH and C=O, respectively [63, 64]. The latter observed peak typically corresponds to the amide I C=O stretching vibration, which is commonly found in the spectral range of 1640–1650 cm<sup>-1</sup> [65]. The observed vibrational peaks in the amide II region for IFN $\alpha/\gamma$  and IFN $\alpha/\gamma$ @PAM<sup>gel</sup> are consistent with the documented natural helical conformation and protein aggregation values previously reported [66]. The swelling behavior of hydrogels plays a pivotal role in biological applications because of its profound impact on diffusion, fluid dynamics, and surface characteristics. The present study successfully demonstrated various characteristics of the hydrogel, which aligns with the findings of previous researchers, who have emphasized the universal applicability of hydrogel carriers [67]. In future studies, we will further investigate strategies to increase the palatability of the hydrogel, prolong its residence time in the duodenum, and extend the duration of IFN action.

The cellular immune response plays a pivotal role in the eradication of viruses and confers protection against viral infections. Although humic acid has a positive effect on animal immune regulation, the effect is limited. Studies have shown that adding humus to chicken diets does not lead to an increase in the proportion of T lymphocytes [68, 69]. However, our results revealed increases in both the CD4<sup>+</sup> and CD8<sup>+</sup> T lymphocyte proportions. Therefore, we further speculate that this effect is caused by rPoIFN $\alpha/\gamma$ . In this study, FCM analysis revealed a significant increase in CD4<sup>+</sup> T lymphocytes following the oral administration of IFN $\alpha/\gamma$ @PAM<sup>gel</sup> (Figure 7I). Various cytokines can induce the differentiation of CD4<sup>+</sup> T cells into distinct subsets of regulatory T cells, including Th1, Th2, and Th17 cells [70]. Moreover, Th1 cells

secrete cytokines, including IFN $\gamma$  and tumor necrosis factor- $\alpha$ , which can stimulate macrophage activation and delay hypersensitivity reactions [71, 72]. Moreover, IFN $\alpha/\gamma$ @PAM<sup>gel</sup> increased the number of CD8<sup>+</sup> T cells (Figure 7J), which are known to play a crucial role in viral clearance [73]. These findings suggest that IFN $\alpha/\gamma$ @PAM<sup>gel</sup> enhances the proliferation of Tc and Th cells in mice. Consequently, we hypothesize that the primary mechanism by which IFN $\alpha/\gamma$ @PAM<sup>gel</sup> exerts its protective effect is through the induction of a robust cellular immune response. The IFN family effectively establishes an antiviral barrier by orchestrating the induction of numerous ISGs and antiviral genes [74]. At present, we have not found a suitable method for real-time detection of IFN release in various tissues. Considering that IFN exerts its antiviral effect mainly by stimulating cells to produce ISGs and that the expression level of ISGs is positively correlated with the content of IFN, we indirectly reflect the release of IFN through changes in the expression level of ISGs. Our findings suggest that the administration of IFN $\alpha/\gamma$ @PAM<sup>gel</sup> can elicit increased expression of PKR, IFIT1, and other antiviral mediators in vivo (Figure 8), which aligns with previous investigations [36, 63]. Therefore, we infer that the release of recombinant PoIFN- $\alpha/\gamma$  in different tissues was greatest at 3–5 days after treatment. Therefore, this may be the primary reason for the increased survival rate and reduced viral load in the IFN $\alpha/\gamma$ @PAM<sup>gel</sup> treatment group (Figure 9A and B). Studies have shown that beneficial systemic effects against different infectious diseases can be achieved when IFNs derived from chickens, mice, cows, sheep, or humans are administered orally [75]. Furthermore, chickens that received chicken IFN- $\alpha$  orally presented more favourable therapeutic outcomes than did those that received it intramuscularly [76]. In this study, oral administration of IFN $\alpha/\gamma$ @PAM<sup>gel</sup> also significantly reduced clinical symptoms and tissue damage in PRV-infected mice (Figures 10A and B). This evidence provides a theoretical basis for oral IFN administration. Our future research will focus on determining the optimal dosage of rPoIFN and enhancing its oral bioavailability.

Overall, a fusion IFN $\alpha/\gamma$  protein that combines the antiviral functions of IFN $\alpha$  and the immunoregulatory functions of IFN $\gamma$  was expressed. A pH-responsive hydrogel loaded with IFN $\alpha/\gamma$  was formulated to withstand the acidic gastric environment and enable controlled release and absorption in the small intestine to facilitate oral administration. The use of this method ameliorated the clinical symptoms exhibited by mice infected with PRV and significantly mitigated their mortality rate. Our findings provide improved solutions for treating PRV and contribute to future research on protein-based drugs. Most importantly, the results indicate

that it may be possible to administer protein-based drugs orally.

## Supplementary Information

The online version contains supplementary material available at <https://doi.org/10.1186/s13567-024-01411-w>.

**Additional file 1: rPoIFN  $\alpha/\gamma$  fusion gene sequence.**

**Additional file 2: Hydrogel porosity. The results of the porosity experiment indicate that the hydrogel has a porosity of approximately 60%.**

**Additional file 3: Experiments on concentration gradients.**

## Acknowledgements

We express our gratitude to all the members of the Veterinary Biologics Team for their valuable suggestions and exceptional technical support.

## Authors' contributions

MS, KZ, YS, BL, and WZ performed the experiments. KZ and WY obtained the resources and designed the experiments. JF and SG supervised the study. MS and KZ analysed the data and drafted the manuscript. All authors read and approved the final manuscript.

## Funding

This study was supported by the Natural Science Foundation of Hebei Province-Biological Agriculture Joint Fund Key Project (Grant No. C2022204249), the National Natural Science Foundation of China (Grant No. 32102644), the Talents Introduction Projects of Hebei Agricultural University (Grant no. YJ201945), and the Science Research Project of Hebei Education Department (QN2024288).

## Availability of data and materials

The data supporting the conclusions of this article are included within the article. The raw data are available upon request.

## Declarations

### Ethics approval and consent to participate

The experiments involving mice were conducted in strict adherence to the principles of biosafety and bioethics, as well as the guidelines provided by the Animal Ethics Committee of Hebei Agricultural University, China (No. 2022145).

### Competing interests

The authors declare that they have no competing interests.

Received: 29 March 2024 Accepted: 16 September 2024

Published online: 20 November 2024

## References

- Liao X, Nie J, Yuan X, Feng Z, Cui E, Wu Y, Li Y, Scherman D, Liu Y (2023) Carbopol dispersed PAA-modified UIO-66 with high colloidal stability as a combination nano-adjuvant boosts immune response and protection against pseudorabies virus in mice and pigs. *Acta Biomater* 168:540–550
- Gou H, Bian Z, Cai R, Chu P, Song S, Li Y, Jiang Z, Zhang K, Yang D, Li C (2021) RIPK3-dependent necroptosis limits PRV replication in PK-15 cells. *Front Microbiol* 12:664353
- Rziha HJ, Mettenleiter TC, Ohlinger V, Wittmann G (1986) Herpesvirus (pseudorabies virus) latency in swine: occurrence and physical state of viral DNA in neural tissues. *Virology* 155:600–613

4. Sun Y, Luo Y, Wang CH, Yuan J, Li N, Song K, Qiu HJ (2016) Control of swine pseudorabies in China: opportunities and limitations. *Vet Microbiol* 183:119–124
5. An TQ, Peng JM, Tian ZJ, Zhao HY, Li N, Liu YM, Chen JZ, Leng CL, Sun Y, Chang D, Tong GZ (2013) Pseudorabies virus variant in Bartha-K61-vaccinated pigs, China, 2012. *Emerg Infect Dis* 19:1749–1755
6. Tong W, Liu F, Zheng H, Liang C, Zhou YJ, Jiang YF, Shan TL, Gao F, Li GX, Tong GZ (2015) Emergence of a pseudorabies virus variant with increased virulence to piglets. *Vet Microbiol* 181:236–240
7. Liu Q, Wang X, Xie C, Ding S, Yang H, Guo S, Li J, Qin L, Ban F, Wang D, Wang C, Feng L, Ma H, Wu B, Zhang L, Dong C, Xing L, Zhang J, Chen H, Yan R, Wang X, Li W (2021) A novel human acute encephalitis caused by pseudorabies virus variant strain. *Clin Infect Dis* 73:e3690–e3700
8. Cai X, Wang Z, Li X, Zhang J, Ren Z, Shao Y, Xu Y, Zhu Y (2023) Emodin as an inhibitor of PRV infection in vitro and in vivo. *Molecules* 28:6567
9. Mantlo E, Bukreyeva N, Maruyama J, Paessler S, Huang C (2020) Antiviral activities of type I interferons to SARS-CoV-2 infection. *Antiviral Res* 179:104811
10. Deng L, Yin Y, Xu Z, Li F, Zhao J, Deng H, Jian Z, Lai S, Sun X, Zhu L (2022) Antiviral activity of porcine IFN- $\lambda$ 3 and IFN- $\alpha$  against porcine rotavirus in vitro. *Molecules* 27:4575
11. Chen SN, Gan Z, Hou J, Yang YC, Huang L, Huang B, Wang S, Nie P (2022) Identification and establishment of type IV interferon and the characterization of interferon- $\nu$  including its class II cytokine receptors IFN- $\nu$ R1 and IL-10R2. *Nat Commun* 13:999
12. Zeuzem S (2004) Heterogeneous virologic response rates to interferon-based therapy in patients with chronic hepatitis C: who responds less well? *Ann Intern Med* 140:370–381
13. Sangewar N, Waghela SD, Yao J, Sang H, Bray J, Mwangi W (2021) Novel potent IFN- $\gamma$ -inducing CD8<sup>+</sup> T cell epitopes conserved among diverse bovine viral diarrhoea virus strains. *J Immunol* 206:1709–1718
14. Platanias LC (2005) Mechanisms of type-I and type-II-interferon-mediated signalling. *Nat Rev Immunol* 5:375–386
15. Fan W, Jiao P, Zhang H, Chen T, Zhou X, Qi Y, Sun L, Shang Y, Zhu H, Hu R, Liu W, Li J (2020) Inhibition of African swine fever virus replication by porcine type I and type II interferons. *Front Microbiol* 11:1203
16. Gao DM, Yu HY, Zhou W, Xia BB, Li HZ, Wang ML, Zhao J (2021) Inhibitory effects of recombinant porcine interferon- $\alpha$  on porcine transmissible gastroenteritis virus infections in TGEV-seronegative piglets. *Vet Microbiol* 252:108930
17. Poupard O, Conti R, Schmocker A, Pancaldi L, Moser C, Nuss KM, Sakar MS, Dobrocky T, Grützmaier H, Mosimann PJ, Pioletti DP (2021) Pulsatile flow-induced fatigue-resistant photopolymerizable hydrogels for the treatment of intracranial aneurysms. *Front Bioeng Biotechnol* 8:619858
18. Chen L, Hu W, Du M, Song Y, Wu Z, Zheng Q (2021) Bioinspired, recyclable, stretchable hydrogel with boundary ultralubrication. *ACS Appl Mater Interfaces* 13:42240–42249
19. Kim J-N, Lee J, Lee H, Oh I-K (2021) Stretchable and self-healable catechol-chitosan-diatom hydrogel for triboelectric generator and self-powered tremor sensor targeting at Parkinson disease. *Nano Energy* 82:105705
20. Verrillo M, Salzano M, Cozzolino V, Spaccini R, Piccolo A (2021) Bioactivity and antimicrobial properties of chemically characterized compost teas from different green composts. *Waste Manag* 120:98–107
21. Verrillo M, Parisi M, Savy D, Caiazzo G, Di Caprio R, Luciano MA, Cacciapuoti S, Fabbrocini G, Piccolo A (2022) Anti-inflammatory activity and potential dermatological applications of characterized humic acids from a lignite and a green compost. *Sci Rep* 12:2152
22. Verrillo M, Savy D, Cangemi S, Savarese C, Cozzolino V, Piccolo A (2022) Valorization of lignins from energy crops and agro-industrial byproducts as antioxidant and antibacterial materials. *J Sci Food Agric* 102:2885–2892
23. Murugesan G, Latha N, Suganya K, Murugan M, Munusamy MA, Rajan M (2018) Stimulus-responsive zinc oxide-functionalized macromolecular humic acid nanocarrier for enhancement of antibacterial activity of ciprofloxacin hydrochloride. *Int J Biol Macromol* 114:1109–1116
24. Ratić G, Chrastrný V, Guinoiseau D, Marsac R, Vaňková Z, Komárek M (2021) Cadmium isotope fractionation during complexation with humic acid. *Environ Sci Technol* 55:7430–7444
25. Venezia V, Matta S, Lehner S, Vitiello G, Costantini A, Gaan S, Malucelli G, Branda F, Luciani G, Bifulco A (2021) Detailed thermal, fire, and mechanical study of silicon-modified epoxy resin containing humic acid and other additives. *ACS Appl Polym Mater* 3:5969–5981
26. Hou M, Yang R, Zhang L, Zhang L, Liu G, Xu Z, Kang Y, Xue P (2018) Injectable and natural humic acid/agarose hybrid hydrogel for localized light-driven photothermal ablation and chemotherapy of cancer. *ACS Biomater Sci Eng* 4:4266–4277
27. Zhang X, Liu W, Yang D, Qiu X (2019) Biomimetic supertough and strong biodegradable polymeric materials with improved thermal properties and excellent UV-blocking performance. *Adv Funct Mater* 29:1806912
28. Wang YJ, Zhang XN, Song Y, Zhao Y, Chen L, Su F, Li L, Wu ZL, Zheng Q (2019) Ultrastiff and tough supramolecular hydrogels with a dense and robust hydrogen bond network. *Chem Mater* 31:1430–1440
29. Criado-Gonzalez M, Iqbal MH, Carvalho A, Schmutz M, Jierry L, Schaaf P, Boulmedais F (2020) Surface triggered self-assembly of Fmoc-tripeptide as an antibacterial coating. *Front Bioeng Biotechnol* 7:938
30. Yu H, Xiao Q, Qi G, Chen F, Tu B, Zhang S, Li Y, Chen Y, Yu H, Duan P (2022) A hydrogen bonds-crosslinked hydrogels with self-healing and adhesive properties for hemostatic. *Front Bioeng Biotechnol* 10:855013
31. Afzal MZ, Yue R, Sun XF, Song C, Wang SG (2019) Enhanced removal of ciprofloxacin using humic acid modified hydrogel beads. *J Colloid Interface Sci* 543:76–83
32. Rubini K, Boanini E, Menichetti A, Bonvicini F, Gentilomi GA, Montalti M, Bigi A (2020) Quercetin loaded gelatin films with modulated release and tailored anti-oxidant, mechanical and swelling properties. *Food Hydrocol* 109:106089
33. Mushtaq F, Raza ZA, Batool SR, Zahid M, Onder OC, Rafique A, Nazeer MA (2022) Preparation, properties, and applications of gelatin-based hydrogels (GHs) in the environmental, technological, and biomedical sectors. *Int J Biol Macromol* 218:601–633
34. Venezia V, Verrillo M, Avallone PR, Silvestri B, Cangemi S, Pasquino R, Grizzuti N, Spaccini R, Luciani G (2023) Waste to wealth approach: improved antimicrobial properties in bioactive hydrogels through humic substance-gelatin chemical conjugation. *Biomacromol* 24:2691–2705
35. Ren J, Wang H, Zhou L, Ge X, Guo X, Han J, Yang H (2020) Glycoproteins C and D of PRV strain HB1201 contribute individually to the escape from Bartha-K61 vaccine-induced immunity. *Front Microbiol* 11:323
36. Jiao P, Wang S, Fan W, Zhang H, Yin H, Shang Y, Zhu H, Liu W, Hu R, Sun L (2023) Recombinant porcine interferon cocktail delays the onset and lessens the severity of African swine fever. *Antiviral Res* 215:105644
37. Meng S, Yang L, Xu C, Qin Z, Xu H, Wang Y, Sun L, Liu W (2011) Recombinant chicken interferon- $\alpha$  inhibits H9N2 avian influenza virus replication in vivo by oral administration. *J Interferon Cytokine Res* 31:533–538
38. Fang J, Zhang Q, Xi Y, Lang L, Wang K, Li S (2023) Analysis of the differential expression and antiviral activity of porcine interferon- $\alpha$  in vitro. *Int J Pept Res Ther* 29:42
39. Cai X, Shao Y, Wang Z, Xu Y, Ren Z, Fu L, Zhu Y (2023) Antiviral activity of dandelion aqueous extract against pseudorabies virus both in vitro and in vivo. *Front Vet Sci* 9:1090398
40. Li SF, Shao JJ, Zhao FR, Gong MJ, Xie YL, Chang HY, Zhang YG (2018) Antiviral activity of porcine interferon delta 8 against foot-and-mouth disease virus in vitro. *Int Immunopharmacol* 59:47–52
41. Wang L, Hao R, Yang Y, Li Y, Lu B, Mao Y, Zhang Y, Gong Z, Liu Y, Qi M, Ru Y, Zheng H (2023) Recombinant porcine interferon-gamma expressed in CHO cells and its antiviral activity. *Sheng Wu Gong Cheng Xue Bao* 39:4784–4795
42. Zhao Y, Xue P, Lin G, Tong M, Yang J, Zhang Y, Ran K, Zhuge D, Yao Q, Xu H (2022) A KPV-binding double-network hydrogel restores gut mucosal barrier in an inflamed colon. *Acta Biomater* 143:233–252
43. Liu X, Steiger C, Lin S, Parada GA, Liu J, Chan HF, Yuk H, Phan NV, Collins J, Tamang S, Traverso G, Zhao X (2019) Ingestible hydrogel device. *Nat Commun* 10:493
44. Zhou J, Wang H, Chen H, Ling Y, Xi Z, Lv M, Chen J (2023) pH-responsive nanocomposite hydrogel for simultaneous prevention of postoperative adhesion and tumor recurrence. *Acta Biomater* 158:228–238
45. Yang Y, Liu Y, Chen S, Cheong KL, Teng B (2020) Carboxymethyl  $\beta$ -cyclodextrin grafted carboxymethyl chitosan hydrogel-based micro-particles for oral insulin delivery. *Carbohydr Polym* 246:116617
46. Mukhopadhyay P, Sarkar K, Chakraborty M, Bhattacharya S, Mishra R, Kundu PP (2013) Oral insulin delivery by self-assembled chitosan

- nanoparticles: in vitro and in vivo studies in diabetic animal model. *Mater Sci Eng C Mater Biol Appl* 33:376–382
47. Neufeld L, Bianco-Peled H (2017) Pectin-chitosan physical hydrogels as potential drug delivery vehicles. *Int J Biol Macromol* 101:852–861
  48. Peng J, Xiao Y, Wan X, Chen Q, Wang H, Li J, Chen J, Gao R (2020) Enhancement of immune response and anti-infection of mice by porcine antimicrobial peptides and interleukin-4/6 fusion gene encapsulated in chitosan nanoparticles. *Vaccines (Basel)* 8:552
  49. Sun Y, Li C, Li Z, Shangguan A, Jiang J, Zeng W, Zhang S, He Q (2021) Quercetin as an antiviral agent inhibits the pseudorabies virus in vitro and in vivo. *Virus Res* 305:198556
  50. Li L, Wang R, Hu H, Chen X, Yin Z, Liang X, He C, Yin L, Ye G, Zou Y, Yue G, Tang H, Jia R, Song X (2021) The antiviral activity of kaempferol against pseudorabies virus in mice. *BMC Vet Res* 17:247
  51. Huang J, Qi Y, Wang A, Huang C, Liu X, Yang X, Li L, Zhou R (2020) Porcine  $\beta$ -defensin 2 inhibits proliferation of pseudorabies virus in vitro and in transgenic mice. *Virology* 17:18
  52. Wang Z, Cai X, Ren Z, Shao Y, Xu Y, Fu L, Zhu Y (2023) Piceatannol as an antiviral inhibitor of PRV infection in vitro and in vivo. *Animals (Basel)* 13:2376
  53. Xie J, Bi Y, Xu S, Han Y, Idris A, Zhang H, Li X, Bai J, Zhang Y, Feng R (2020) Host antiviral protein IFITM2 restricts pseudorabies virus replication. *Virus Res* 287:198105
  54. Cheng H, Wu H, Guo T, Jin Park H, Li J (2022) Zinc insulin hexamer loaded alginate zinc hydrogel: preparation, characterization and in vivo hypoglycemic ability. *Eur J Pharm Biopharm* 179:173–181
  55. Phan VH, Mathiyalagan R, Nguyen MT, Tran TT, Murugesan M, Ho TN, Huong H, Yang DC, Li Y, Thambi T (2022) Ionically cross-linked alginate-chitosan core-shell hydrogel beads for oral delivery of insulin. *Int J Biol Macromol* 222:262–271
  56. Song B, Wei W, Liu X, Huang Y, Zhu S, Yi L, Eerdunfu DH, Zhao M, Chen J (2023) Recombinant porcine interferon- $\alpha$  decreases pseudorabies virus infection. *Vaccines (Basel)* 11:1587
  57. Zhao J, Zhu L, Xu L, Huang J, Sun X, Xu Z (2020) Porcine interferon lambda 3 (IFN- $\lambda$ 3) shows potent anti-PRRSV activity in primary porcine alveolar macrophages (PAMs). *BMC Vet Res* 16:408
  58. Zhang T, Liu Y, Chen Y, Wang J, Feng H, Wei Q, Zhao S, Yang S, Ma H, Liu D, Zhang G (2021) Antiviral activity of porcine interferon delta 8 against pseudorabies virus in vitro. *Int J Biol Macromol* 177:10–18
  59. Zhao K, Li X, Lei B, Han Y, An T, Zhang W, Zhang H, Li B, Yuan W (2023) Recombinant porcine interferon- $\alpha$  and interleukin-2 fusion protein (rPolIFN $\alpha$ +IL-2) shows potent anti-pseudorabies virus activity in vitro and in vivo. *Vet Microbiol* 279:109678
  60. Ho TC, Chang CC, Chan HP, Chung TW, Shu CW, Chuang KP, Duh TH, Yang MH, Tyan YC (2022) Hydrogels: properties and applications in biomedicine. *Molecules* 27:2902
  61. Huynh CT, Nguyen MK, Lee DS (2011) Biodegradable pH/temperature-sensitive oligo( $\beta$ -amino ester urethane) hydrogels for controlled release of doxorubicin. *Acta Biomater* 7:3123–3130
  62. Hou M, Liu W, Zhang L, Zhang L, Xu Z, Cao Y, Kang Y, Xue P (2020) Responsive agarose hydrogel incorporated with natural humic acid and MnO<sub>2</sub> nanoparticles for effective relief of tumor hypoxia and enhanced photo-induced tumor therapy. *Biomater Sci* 8:353–369
  63. Pedrosa-Santana S, Lamazares Arcia E, Fleitas-Salazar N, Gancino Guevara M, Mansilla R, Gómez-Gaete C, Altamirano C, Fernandez K, Ruiz A, Toledo Alonso JR (2020) Polymeric nanoencapsulation of alpha interferon increases drug bioavailability and induces a sustained antiviral response in vivo. *Mater Sci Eng C Mater Biol Appl* 116:111260
  64. Gupta MK, Vanwert A, Bogner RH (2003) Formation of physically stable amorphous drugs by milling with neusilin. *J Pharm Sci* 92:536–551
  65. Zha K, Xiong Y, Zhang W, Tan M, Hu W, Lin Z, Cheng P, Lu L, Cai K, Mi B, Feng Q, Zhao Y, Liu G (2023) Waste to wealth: near-infrared/pH dual-responsive copper-humic acid hydrogel films for bacteria-infected cutaneous wound healing. *ACS Nano* 17:17199–17216
  66. Ami D, Natalello A, Taylor G, Tonon G, Maria Doglia S (2006) Structural analysis of protein inclusion bodies by fourier transform infrared microspectroscopy. *Biochim Biophys Acta* 1764:793–799
  67. Zhang N, Zhang C, Liu J, Fan C, Yin J, Wu T (2022) An oral hydrogel carrier for delivering resveratrol into intestine-specific target released with high encapsulation efficiency and loading capacity based on structure-selected alginate and pectin. *Food Funct* 13:12051–12066
  68. Mudroňová D, Karaffová V, Semjon B, Nad P, Koščová J, Bartkovský M, Makiš A, Bujňák L, Nagy J, Mojžišová J, Marcinčák S (2021) Effects of dietary supplementation of humic substances on production parameters, immune status and gut microbiota of laying hens. *Agriculture* 11:744
  69. Mudroňová D, Karaffová V, Pešulová T, Koščová J, Maruščáková IC, Bartkovský M, Marcinčáková D, Ševčíková Z, Marcinčák S (2020) The effect of humic substances on gut microbiota and immune response of broilers. *Food Agr Immunol* 31:137–149
  70. Owen KL, Brockwell NK, Parker BS (2019) JAK-STAT Signaling: a double-edged sword of immune regulation and cancer progression. *Cancers (Basel)* 11:2002
  71. Abbas AK, Murphy KM, Sher A (1996) Functional diversity of helper T lymphocytes. *Nature* 383:787–793
  72. Mosmann TR, Coffman RL (1989) Heterogeneity of cytokine secretion patterns and functions of helper T cells. *Adv Immunol* 46:111–147
  73. Ren X, Cao N, Tian L, Liu W, Zhu H, Rong Z, Yao M, Li X, Qian P (2023) A self-assembled nanoparticle vaccine based on pseudorabies virus glycoprotein D induces potent protective immunity against pseudorabies virus infection. *Vet Microbiol* 284:109799
  74. Huang H, Zhang N, Xiong Q, Chen R, Zhang C, Wang N, Wang L, Ren H, Liu M, Qian M, Du B (2017) Elimination of GPR146-mediated antiviral function through IRF3/HES1-signalling pathway. *Immunology* 152:102–114
  75. Cummins JM, Krakowka GS, Thompson CG (2005) Systemic effects of interferons after oral administration in animals and humans. *Am J Vet Res* 66:164–176
  76. Anjum FR, Rahman SU, Aslam MA, Qureshi AS (2020) Comparative study of protection against Newcastle disease in young broilers administered natural chicken alpha interferon via oral and intramuscular routes. *mSphere* 5:e00585–20

## Publisher's Note

Springer Nature remains neutral with regard to jurisdictional claims in published maps and institutional affiliations.